

MNI C-terminal truncation syndrome is a novel neurodevelopmental and craniofacial disorder with partial rhombencephalosynapsis

Christopher C.Y. Mak,^{1,*} Dan Doherty,^{2,3,*} Angela E. Lin,⁴ Nancy Vegas,^{5,6} Megan T. Cho,⁷ Géraldine Viot,⁸ Clémantine Dimartino,^{5,6} James D. Weisfeld-Adams,^{9,†}  Davor Lessel,¹⁰ Shelagh Joss,¹¹ Chumei Li,¹² Claudia Gonzaga-Jauregui,¹³ Yuri A. Zarate,¹⁴ Nadja Ehmke,¹⁵ Denise Horn,¹⁵ Caitlin Troyer,¹⁶ Sarina G. Kant,¹⁷ Youngha Lee,¹⁸ Gisele E. Ishak,^{3,19} Gordon Leung,¹ Amanda Barone Pritchard,²⁰ Sandra Yang,⁷ Eric G. Bend,^{21,22}  Francesca Filippini,^{5,6} Chelsea Roadhouse,¹² Nicolas Lebrun,²³ Michele G. Mehaffey,² Pierre-Marie Martin,^{24,25} Benjamin Apple,⁹ Francisca Millan,⁷ Oliver Puk,²⁶ Mariette J.V. Hoffer,¹⁷ Lindsay B. Henderson,⁷ Ruth McGowan,¹¹ Ingrid M. Wentzensen,⁷ Steven Pei,¹ Farah R. Zahir,²⁷ Mullin Yu,¹ William T. Gibson,²⁷ Ann Seman,²⁸ Marcie Steeves,⁴ Jill R. Murrell,²⁹ Sabine Luetzgen,¹⁰ Elizabeth Francisco,³⁰ Tim M. Strom,^{31,32} Louise Amlie-Wolf,³³ Angela M. Kaindl,^{34,35} William G. Wilson,¹⁶ Sara Halbach,³⁶ Lina Basel-Salmon,^{37,38,39,40} Noa Lev-El,³⁷ Jonas Denecke,⁴¹ Lisenka E.L.M. Vissers,⁴² Kelly Radtke,⁴³ Jamel Chelly,^{44,45,46} Elaine Zackai,^{20,47} Jan M. Friedman,²⁷ Michael J. Bamshad,^{2,48,49} Deborah A. Nickerson,^{48,49} University of Washington Center for Mendelian Genomics,⁴⁹ Russell R. Reid,⁵⁰ Koenraad Devriendt,⁵¹ Jong-Hee Chae,⁵² Elliot Stolerman,²¹ Carey McDougall,²⁰ Zöe Powis,⁴³ Thierry Bienvenu,^{23,53}  Tiong Y. Tan,⁵⁴ Naama Orenstein,^{38,39} William B. Dobyns,^{2,3,55} Joseph T. Shieh,^{24,25} Murim Choi,^{18,52} Darrel Waggoner,³⁶ Karen W. Gripp,³³ Michael J. Parker,⁵⁶ Joan Stoler,²⁸ Stanislas Lyonnet,^{5,6,57} Valérie Cormier-Daire,^{6,57,58} David Viskochil,⁵⁹ Trevor L. Hoffman,⁶⁰ Jeanne Amiel,^{5,6,57} Brian H.Y. Chung^{1,*} and  Christopher T. Gordon^{5,6,*}

*These authors contributed equally to this work.

†Deceased.

MNI encodes a transcriptional co-regulator without homology to other proteins, previously implicated in acute myeloid leukaemia and development of the palate. Large deletions encompassing *MNI* have been reported in individuals with variable neurodevelopmental anomalies and non-specific facial features. We identified a cluster of *de novo* truncating mutations in *MNI* in a cohort of 23 individuals with strikingly similar dysmorphic facial features, especially midface hypoplasia, and intellectual disability with severe expressive language delay. Imaging revealed an atypical form of rhombencephalosynapsis, a distinctive brain malformation characterized by partial or complete loss of the cerebellar vermis with fusion of the cerebellar hemispheres, in 8/10 individuals. Rhombencephalosynapsis has no previously known definitive genetic or environmental causes. Other frequent features included perisylvian polymicrogyria, abnormal posterior clinoid processes and persistent trigeminal artery. *MNI* is encoded by only two exons. All mutations, including the recurrent variant p.Arg1295* observed in 8/21 probands, fall in the terminal exon or the extreme 3' region of exon 1, and are therefore predicted to result in escape from nonsense-mediated mRNA decay. This was

Received July 5, 2019. Revised October 2, 2019. Accepted October 15, 2019. Advance Access publication December 13, 2019

© The Author(s) (2019). Published by Oxford University Press on behalf of the Guarantors of Brain. All rights reserved.

For permissions, please email: journals.permissions@oup.com

confirmed in fibroblasts from three individuals. We propose that the condition described here, MN1 C-terminal truncation (MCTT) syndrome, is not due to *MN1* haploinsufficiency but rather is the result of dominantly acting C-terminally truncated MN1 protein. Our data show that *MN1* plays a critical role in human craniofacial and brain development, and opens the door to understanding the biological mechanisms underlying rhombencephalosynapsis.

- 1 Department of Paediatrics and Adolescent Medicine, LKS Faculty of Medicine, The University of Hong Kong, Hong Kong Special Administrative Region, China
- 2 Department of Pediatrics, University of Washington, Seattle, WA 98195, USA
- 3 Center for Integrative Brain Research, Seattle Children's Research Institute, Seattle, WA 98101, USA
- 4 Medical Genetics, MassGeneral Hospital for Children, Boston, MA 02114, USA
- 5 Laboratory of Embryology and Genetics of Human Malformation, Institut National de la Santé et de la Recherche Médicale (INSERM) UMR 1163, Institut Imagine, 75015 Paris, France
- 6 Paris Descartes-Sorbonne Paris Cité University, Institut Imagine, 75015 Paris, France
- 7 GeneDx, Gaithersburg, MD 20877, USA
- 8 Gynécologie Obstétrique, Hôpital Cochin, Hôpitaux Universitaires Paris Centre (HUPC), Assistance Publique Hôpitaux de Paris (AP-HP), 75014 Paris, France
- 9 Section of Clinical Genetics and Metabolism, Department of Pediatrics, University of Colorado-Denver School of Medicine, Aurora, CO 80045, USA
- 10 Institute of Human Genetics, University Medical Center Hamburg-Eppendorf, 20246 Hamburg, Germany
- 11 West of Scotland Regional Genetics Service, Queen Elizabeth University Hospital, Glasgow G51 4TF, UK
- 12 McMaster University Medical Center, Hamilton, Ontario, Canada
- 13 Regeneron Genetics Center, Regeneron Pharmaceuticals Inc, Tarrytown, NY 10591, USA
- 14 Section of Genetics and Metabolism, University of Arkansas for Medical Sciences, Arkansas Children's Hospital, Little Rock, AR 72202, USA
- 15 Institute for Medical Genetics and Human Genetics, Charité – Universitätsmedizin Berlin, 13353 Berlin, Germany
- 16 Pediatrics and Medical Genetics, University of Virginia Health System, Charlottesville, VA, USA
- 17 Department of Clinical Genetics, Leiden University Medical Center, 2300 RC Leiden, The Netherlands
- 18 Department of Biomedical Sciences, Seoul National University College of Medicine, Seoul, Republic of Korea
- 19 Department of Radiology, University of Washington, Seattle, WA 98195, USA
- 20 Division of Human Genetics, Children's Hospital of Philadelphia, Philadelphia, PA 19104, USA
- 21 Greenwood Genetic Center, Greenwood, SC 29646, USA
- 22 PreventionGenetics, Marshfield, WI 54449, USA
- 23 Institut Cochin, INSERM U1016, CNRS UMR 8104, Paris Descartes University, 75014 Paris, France
- 24 Institute for Human Genetics, University of California San Francisco, San Francisco, CA, USA
- 25 Division of Medical Genetics, Department of Pediatrics, University of California San Francisco, San Francisco, CA, USA
- 26 Praxis für Humangenetik Tübingen, 72076 Tübingen, Germany
- 27 Department of Medical Genetics, University of British Columbia, Vancouver, BC, V6T 1Z4, Canada
- 28 Division of Genetics and Genomics, Boston Children's Hospital, Boston, MA 02115, USA
- 29 Division of Genomic Diagnostics, Children's Hospital of Philadelphia, Philadelphia, PA 19104, USA
- 30 eviCore healthcare, Bluffton, SC 29910, USA
- 31 Institute of Human Genetics, Helmholtz Zentrum München, 85764 Neuherberg, Germany
- 32 Institute of Human Genetics, Technische Universität München, 81675 Munich, Germany
- 33 Division of Medical Genetics, A I duPont Hospital for Children/Nemours, Wilmington, DE 19803, USA
- 34 Charité – Universitätsmedizin Berlin, Institute of Neuroanatomy and Cell Biology, Department of Pediatric Neurology and Center for Chronically Sick Children, Berlin, Germany
- 35 Berlin Institute of Health (BIH), Berlin, Germany
- 36 Department of Human Genetics, University of Chicago, Chicago, IL, USA
- 37 Raphael Recanati Genetic Institute, Rabin Medical Center–Beilinson Hospital, Petach Tikva, Israel
- 38 Pediatric Genetics Clinic, Schneider Children's Medical Center of Israel, Petach Tikva, Israel
- 39 Sackler Faculty of Medicine, Tel Aviv University, Tel Aviv, Israel
- 40 Felsenstein Medical Research Center, Petach Tikva, Israel
- 41 Department of Pediatrics, University Medical Center Hamburg-Eppendorf, 20246 Hamburg, Germany
- 42 Department of Human Genetics, Donders Centre for Neuroscience, Radboud University Medical Center, PO Box 9101, 6500 HB Nijmegen, The Netherlands
- 43 Clinical Genomics Department, Ambry Genetics, Aliso Viejo, CA 92656, USA
- 44 Laboratoire de Diagnostic Génétique, Hôpitaux Universitaires de Strasbourg, Nouvel Hôpital Civil, 67091 Strasbourg, France
- 45 Fédération de Médecine Translationnelle de Strasbourg, Université de Strasbourg, 67000 Strasbourg, France
- 46 Institut de Génétique et de Biologie Moléculaire et Cellulaire, INSERM U964, CNRS UMR7104, Université de Strasbourg, 67404 Illkirch, France

- 47 Department of Pediatrics, Perelman School of Medicine at the University of Pennsylvania, Philadelphia, PA 19104, USA
48 Department of Genome Sciences, University of Washington, Seattle, WA 98195, USA
49 University of Washington Center for Mendelian Genomics, Seattle, WA 98195, USA
50 Department of Surgery, Section of Plastic Surgery, University of Chicago, Chicago, IL, USA
51 Department of Human Genetics, Katholieke Universiteit Leuven, 3000 Leuven, Belgium
52 Department of Pediatrics, Seoul National University College of Medicine, Seoul, Republic of Korea
53 Laboratoire de Génétique et Biologie Moléculaires, Hôpital Cochin, HUPC, AP-HP, 75014 Paris, France
54 Victorian Clinical Genetics Services, Murdoch Children's Research Institute, Department of Paediatrics, University of Melbourne, Melbourne, 3052, Australia
55 Department of Neurology, University of Washington, Seattle, WA 98195, USA
56 Sheffield Clinical Genetics Service, Sheffield Children's Hospital, Sheffield S10 2TH, UK
57 Département de Génétique, Hôpital Necker-Enfants Malades, AP-HP, 75015 Paris, France
58 Laboratory of Molecular and Physiopathological Bases of Osteochondrodysplasia, INSERM UMR 1163, Institut Imagine, 75015 Paris, France
59 Division of Medical Genetics, University of Utah, Salt Lake City, UT 84132, USA
60 Southern California Kaiser Permanente Medical Group, Anaheim, CA 92801, USA

Correspondence to: Christopher T. Gordon

Laboratory of Embryology and Genetics of Human Malformation, Institut National de la Santé et de la Recherche Médicale (INSERM) UMR 1163, Institut Imagine, 75015 Paris, France

E-mail: chris.gordon@inserm.fr

Correspondence may also be addressed to: Brian H.Y. Chung

Department of Paediatrics and Adolescent Medicine, LKS Faculty of Medicine, The University of Hong Kong, Hong Kong Special Administrative Region, China

E-mail: bhychung@hku.hk

Keywords: MN1; MCTT syndrome; craniofacial development; intellectual disability; rhombencephalosynapsis

Abbreviations: MCTT = MN1 C-terminal truncation; RES = rhombencephalosynapsis; WES = whole exome sequencing

Introduction

The use of trio whole exome sequencing (WES) has dramatically increased our ability to provide a molecular diagnosis for individuals with sporadic developmental disorders (Deciphering Developmental Disorders Study, 2015). Recently, global data exchange platforms such as GeneMatcher have been created to facilitate the validation of suspected disease-causing variants, identified predominantly by WES, in rare disorders (Sobreira *et al.*, 2015). Despite the success of these approaches, the genetic causes of many presumed Mendelian conditions remain elusive. Rhombencephalosynapsis (RES), a brain malformation characterized by total or partial absence of the cerebellar vermis with apparent fusion of the cerebellar hemispheres is one of these conditions (Ishak *et al.*, 2012). Individuals with RES have prominent neurodevelopmental features including motor delays, abnormal eye movements, stereotypies, hyperactivity, executive dysfunction, and a broad range of cognitive ability that correlates somewhat with the degree of RES on imaging (Ishak *et al.*, 2012; Tully *et al.*, 2013). Syndromic associations with RES have been reported (Tully *et al.*, 2012), including Gomez-Lopez-Hernandez syndrome (MIM 601853) and VACTERL association (MIM 192350); however, no definitive genetic causes of RES have been identified (Aldinger *et al.*, 2018).

Here, we report the use of 'genotype-first' approaches for the identification of clustered C-terminal truncating mutations in MN1 proto-oncogene, transcriptional regulator (MN1; MIM 156100) as the cause of a highly recognizable neurodevelopmental disorder with distinctive craniofacial features. Although large chromosomal deletions of a region including this gene has been reported in patients with variable developmental delay, a distinct phenotype is evident in patients with C-terminal truncating mutations. Furthermore, systematic review of the brain imaging for individuals with MN1 C-terminal truncating mutations revealed a highly characteristic pattern of brain malformation, including a focal variant of RES, thus shedding light on a poorly understood brain malformation.

Materials and methods

Comparative genomic hybridization, and whole exome and genome sequencing

WES or whole genome sequencing (WGS) was performed for 25 individuals with undiagnosed, syndromic intellectual disability or developmental delay and dysmorphic facial

features in 15 independent research or diagnostic laboratories. WES was performed using methods described previously as follows: Strauss *et al.* (2018) for Individual 1; Poirier *et al.* (2017) for Individual 3; Choi *et al.* (2009) for Individual 9; Lelieveld *et al.* (2016) for Individual 10; Farwell *et al.* (2015) for Individual 13; Deciphering Developmental Disorders Study, (2017) for Individuals 16 and 19; Hempel *et al.* (2015) for Individual 20; Van De Weghe *et al.* (2017) for Individual 21 and Louie *et al.* (2017) for Individual 24. For Individual 15, Medical Exome sequencing was performed by EGL Genetics. Clinical WGS was performed for Individual 18 using 2×150 bp reads on an Illumina sequencer, with a mean coverage of $30\times$ in the target region. For Individuals 4–7, 11, 12, 14, 17, 23 and 25, WES was performed by GeneDx, as follows. Using genomic DNA from the proband and parents, exonic regions and flanking splice junctions were captured using the Clinical Research Exome kit (Agilent Technologies), the SureSelect Human All Exon V4 (50 Mb) kit or the IDT xGen Exome Research Panel v1.0 and sequenced on an Illumina system with ≥ 100 bp paired-end reads. Reads were aligned to human genome build GRCh37/UCSC hg19, and analysed for sequence variants using a custom-developed analysis tool. Additional sequencing technology and variant interpretation protocols used by GeneDx have been previously described (Tanaka *et al.*, 2015). The general assertion criteria for variant classification by GeneDx are publicly available on the GeneDx ClinVar submission page. WES for Individuals 8 and 22 was performed using Illumina sequencing followed by standard protocols for read mapping and variant calling. WES for Individual 26 was performed using the Agilent SureSelectXT Human all Exon v5 capture kit followed by sequencing on a NextSeq 500 (Illumina) and analysed using an in-house sequence analysis pipeline (Modular GATK-Based Variant Calling Pipeline, MAGPIE), with LOVDplus (Leiden Genome Technology Center, LUMC, Leiden) used for interpretation of variants. The deletion in Individual 27 was identified by array comparative genomic hybridization (CGH) using peripheral blood DNA on the Cytochip Oligo 4x180K v1.0 (Fa. Illumina/Bluegenome) and confirmed by qPCR with primers covering the deleted 22q region. The deletion in Individual 28 (Patient 7807 in Friedman *et al.*, 2006, 2009) was identified using an Affymetrix 100K CGH platform (Friedman *et al.*, 2006) and the breakpoints refined on an Affymetrix 500K platform (Friedman *et al.*, 2009). Genetic research was performed according to approved institutional ethical guidelines and consent was obtained from all families.

cDNA sequencing and real-time PCR

For Individual 2, RNA was extracted from cultured fibroblasts using an RNeasy[®] Mini Kit (Qiagen) and cDNA was generated with a Verso[™] cDNA Synthesis Kit (Thermo Scientific). For Individual 10, cDNA was generated from TRIzol[®]-extracted fibroblast RNA using the SuperScript[™] III First-Strand Synthesis System (Invitrogen). *MNI* cDNA was amplified by PCR using a sense primer in exon 1 and an antisense primer in exon 2 followed by Sanger sequencing. Real-time PCR for Individual 10 was performed in a 7900HT Fast Real-Time PCR System with Fast 96-Well Block Module, using PrimeTime qPCR primer and probe-based assays (Integrated DNA Technologies), with wild-type and mutant

c.3870_3879dup *MNI* probes specific to each sequence. See Supplementary Table 2 for primer and probe sequences.

RNA sequencing

For RNA-Seq of skin fibroblasts from Individual 10, libraries were constructed using Illumina TruSeq RNA sample Prep Kit v2, and sequenced on an Illumina HiSeq 2500. Trimmed FASTQ files were aligned to the NCBI RefSeq human reference genome (GRCh37/hg19) and human transcriptome by Strand NGS software (Strand Life Sciences Private Limited) based on the COBWEB aligner with a gap percentage of 15 bp. Variants with a minimum base quality and mapping quality of 20 were then called by Strand NGS software to obtain all variants in the *MNI* gene. For RNA-Seq of fibroblasts from Individual 21, total RNA was extracted using TRIzol[®] and purified with an RNA Clean & Concentrator-5 kit (Zymo Research). Libraries were prepared using a TruSeq Stranded mRNA kit and sequenced on an Illumina NovaSeq instrument, yielding 100 bp paired-end reads. Trimmed fastq files were processed according to GATK's RNA-Seq best practices and aligned to the human reference genome (GRCh37/hg19) using the two-pass method of STAR (v2.5).

Data availability

Raw data are available upon reasonable request.

Results

Identification of C-terminal truncating variants in *MNI*

Twenty-two probands sequenced by WES or WGS (Individuals 1, 3, 4, and 8–26) harboured *de novo* predicted protein-truncating (stop or frameshift) variants in *MNI* (Fig. 1, Supplementary Fig. 1 and Supplementary Table 1). Because of strong clinical similarities noted between Individual 2 and other probands in the cohort, we performed Sanger sequencing of *MNI* in Individual 2, and identified the variant p.(Glu1249*), which was absent in the father (the mother was unavailable for testing). Individual 7 is the mildly affected father of affected siblings (Individuals 5 and 6). The mutation p.(Gln1273*) was present in all three by WES, but with wild-type:mutant read imbalance in the father (137:87), and Sanger sequencing of blood DNA further supported somatic mosaicism of the variant in the father (Supplementary Fig. 2). The *MNI* gene comprises two exons and encodes a protein of 1320 amino acids. The large first exon codes for amino acids 1–1260 and the second encodes the remaining 60 C-terminal amino acids. All truncating variants in Individuals 1–23 are located within the second exon or at the extreme 3' end of exon 1 (Fig. 1). Individuals 24–26 harboured *de novo* truncating mutations in a much more N-terminal region of *MNI* (Fig. 1), and did not display dysmorphic facial features typical of those patients with C-terminal truncations (see below). None of the above *MNI* variants have been

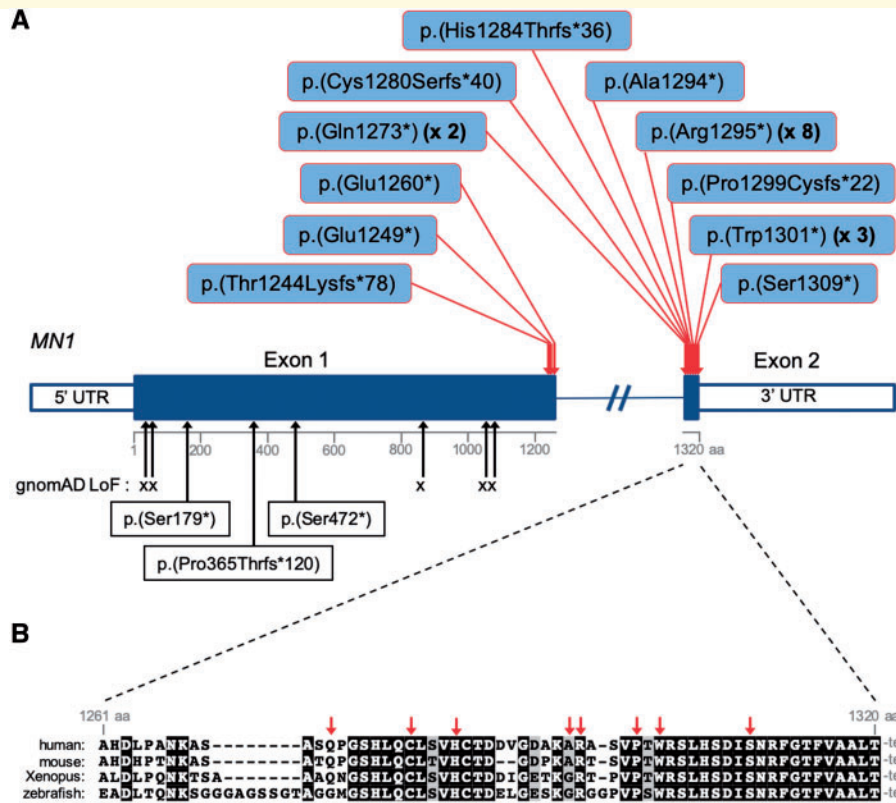


Figure 1 MN1 mutations and sequence conservation. (A) Distribution of C-terminal truncating mutations identified in *MN1* in 21 probands (red arrows). Beneath the schema of the gene, black arrows indicate the positions of loss-of-function variants in the gnomAD database and p.(Ser179*), p.(Pro365Thrfs*120) and p.(Ser472*) identified in Individuals 24, 25 and 26, respectively. (B) *MN1* C-terminal sequence conservation. Multi-species sequence alignment of the entire exon 2 coding region of *MN1*. Sequences were obtained from the following RefSeq or Ensembl transcripts: human, NM_002430.2; mouse, NM_001081235.1; *Xenopus*, NM_001100202.1; zebrafish, ENSDART00000129197. Red arrows indicate the positions of the mutations identified in exon 2.

reported in the Genome Aggregation Database (gnomAD; data accessed May 2019). Given that all the variants in Individuals 1–23 create premature stop codons in the final exon or the final 37 nucleotides of exon 1, all are predicted to result in *MN1* transcripts that escape nonsense-mediated mRNA decay, given the rule that premature stop codons more than 50–55 nucleotides upstream of the final exon-exon junction trigger nonsense-mediated mRNA decay (Nagy and Maquat, 1998). cDNA sequencing, real-time PCR and/or RNA-Seq demonstrated expression of the mutant transcript at levels similar to that of wild-type in cultured fibroblasts from Individual 2 (harbouring a premature stop codon within the 3' terminus of exon 1) and Individuals 10 and 21 (harbouring premature stops in exon 2) (Supplementary Figs 3 and 4). These results suggest that the *MN1* variants identified in Individuals 1–23 may lead to the expression of C-terminally truncated protein with pathogenic effect. Unique phenotypes associated with C-terminal truncating mutations that escape nonsense-mediated mRNA decay have similarly been reported for several genes (White *et al.*, 2016; Jansen *et al.*, 2017). Strikingly, 8 of 21 probands with C-terminal truncations harboured an identical *MN1* variant, p.(Arg1295*),

suggesting a mutational hotspot (Fig. 1). This bias may at least in part be due to underlying nucleotide composition; p.(Arg1295*) is generated from a C to T transition at a CpG dinucleotide. This mutational signature is overrepresented among human germline mutations (Acuna-Hidalgo *et al.*, 2016), and there are no other CpGs with potential to generate a stop codon by C to T transition in exon 2 or in the final 55 nucleotides of exon 1 of *MN1*.

Clinical features in individuals with *MN1* C-terminal truncating variants

The major clinical features and their frequencies for individuals with C-terminal truncations in *MN1* (Individuals 1–6 and 8–23; Individual 7 was not included in the phenotype frequency analysis because of mosaicism of the mutation) are summarized in Table 1 and all available clinical details are provided in Supplementary Table 1. While complete clinical data were not available for all individuals, neurodevelopmental deficits were frequent, with intellectual disability present in 16/17 patients and delayed or absent expressive speech in 18/20. Gross motor development was

delayed in 19/20 cases. Hypotonia was frequent ($n = 17/18$) and feeding difficulties occurred in 12/18. Non-standardized photographs were reviewed for all except Individuals 1, 8, 9 and 15, revealing a distinctive facial gestalt, characterized by midface hypoplasia ($n = 21/22$), hypertelorism ($n = 19/21$), downslanting palpebral fissures ($n = 15/21$) and a short, upturned nose especially in infancy ($n = 21/22$) (Fig. 2). Skull shape anomalies were frequent ($n = 16/21$), and consisted of brachycephaly, plagiocephaly, turriccephaly, dolicocephaly and/or bi-temporal narrowing, with craniosynostosis documented in three individuals (Fig. 3). Mild exorbitism, suggesting shallow orbits, was apparent in the majority of patients, and there was a trend for frontal bossing in infancy and a tall forehead at later ages. A high-arched palate occurred in 15/21 patients (Fig. 2). Only one patient had a cleft palate (submucous), which was associated with a bifid uvula. Ear anomalies were present in 22/22 patients and included low-set, posteriorly-rotated and/or small ears, with the upper portion of the pinna frequently dysplastic (Supplementary Fig. 5). Hearing loss, conductive or sensorineural, occurred in 16/20 individuals. Anomalies occurring in a minority of the 22 patients included: oculomotor defects in nine (including Duane anomaly, nystagmus and strabismus); spinal anomalies, either clinical (lordosis, scoliosis, kyphosis) or radiographic, in eight; atrial or ventricular septal defects in six; seizures in six; and congenital diaphragmatic hernia in two. Growth parameters tended to remain within the normal range. Individual 7 carrying a mosaic *MN1* mutation did not have major neurodevelopmental or craniofacial anomalies other than mildly dysplastic ears and a high palate. The identification of a truncating variant in *MN1* in Individual 2, who was tested because of clinical similarities with other individuals in the series, demonstrates the

recognizability of this disorder. A computational composite created through the Face2Gene application (Gurovich *et al.*, 2019) using multiple patient photos highlights the facial gestalt (Supplementary Fig. 6). We name this condition MN1 C-terminal truncation (MCTT) syndrome.

Brain imaging features in individuals with MN1 C-terminal truncating variants

Initial clinical interpretation of brain MRIs from MCTT syndrome patients identified varied anomalies in several individuals, including polymicrogyria, dysmorphic corpus callosum and anomalies of the cerebellum. Prior to detection of the *de novo* variant in *MN1*, Individual 21 had a long-standing diagnosis of RES. This prompted detailed review of the brain imaging for 11 individuals in the cohort by D.D., G.I. and W.B.D., revealing a highly characteristic pattern of brain malformation (Table 2). Eight of ten patients had focal crossing of the cerebellar folia with loss of vermis morphology consistent with a partial form of RES (Fig. 4). The most extensive involvement resembles more classic partial RES but without fusion of the central white matter or complete loss of vermis landmarks on sagittal view. In addition, 9/10 individuals had polymicrogyria of the insula, which sometimes extended more broadly in the perisylvian region. Similar to other individuals with RES, 3/11 had ventriculomegaly (one shunted), and 4/8 had hypoplastic olfactory bulbs. In contrast to other individuals with RES, 6/11 MCTT patients had above average thickness of the rostral corpus callosum and none had absent septum, although one had a cavum velum interpositum (Fig. 4C, Individual 14). We also noted a persistent medial primitive trigeminal artery in 7/10 (six unilateral, one bilateral), often associated with prominent posterior clinoid processes that sometimes were fused across the midline (Figs 4 and 5). Persistent trigeminal artery is an embryonic connection between the anterior and posterior cerebral circulation that has been detected in 0.1–0.6% of individuals undergoing vascular imaging (O'uchi and O'uchi, 2010), so the 70% prevalence in association with *MN1* variants is far greater than expected by chance. The pituitary did not appear abnormal in any of the patients.

Impact of MN1 N-terminal truncating variants and whole gene deletions

The clustering of *de novo* truncating mutations at the C-terminus of *MN1*, associated with a specific phenotype, is suggestive of a pathogenic effect of the mutations that is not equivalent to haploinsufficiency. We investigated individuals with other types of lesions at the *MN1* locus in order to provide support for this argument, and thereby to establish specific genotype-phenotype relationships. In gnomAD, which is composed of variants identified in

Table 1 Frequency of major clinical findings associated with C-terminal truncations of *MN1*

Phenotype	Affected individuals, n (%)
Hypertelorism	19/21 (90)
Downslanting palpebral fissures	15/21 (71)
Midface hypoplasia	21/22 (95)
Cranial shape defects (plagiocephaly, brachycephaly, turriccephaly, dolicocephaly, bitemporal narrowing)	16/21 (76)
Short, upturned nose	21/22 (95)
High-arched palate	15/21 (71)
Dysplastic ears	22/22 (100)
Hearing loss (conductive or sensorineural)	16/20 (80)
Speech delay	18/20 (90)
Intellectual disability	16/17 (94)
Motor delay	19/20 (95)
Feeding difficulties	12/18 (67)
Hypotonia	17/18 (94)

Note that only Individuals 1–6 and 8–23 were considered for the frequencies listed (Individual 7 was excluded because mosaicism of the *MN1* mutation).



Figure 2 Facial features of individuals with C-terminal truncating mutations in MNI. Oral view for Individuals 18 and 22 indicates high and narrow palate. Individual identification numbers are indicated at the top left of each panel.

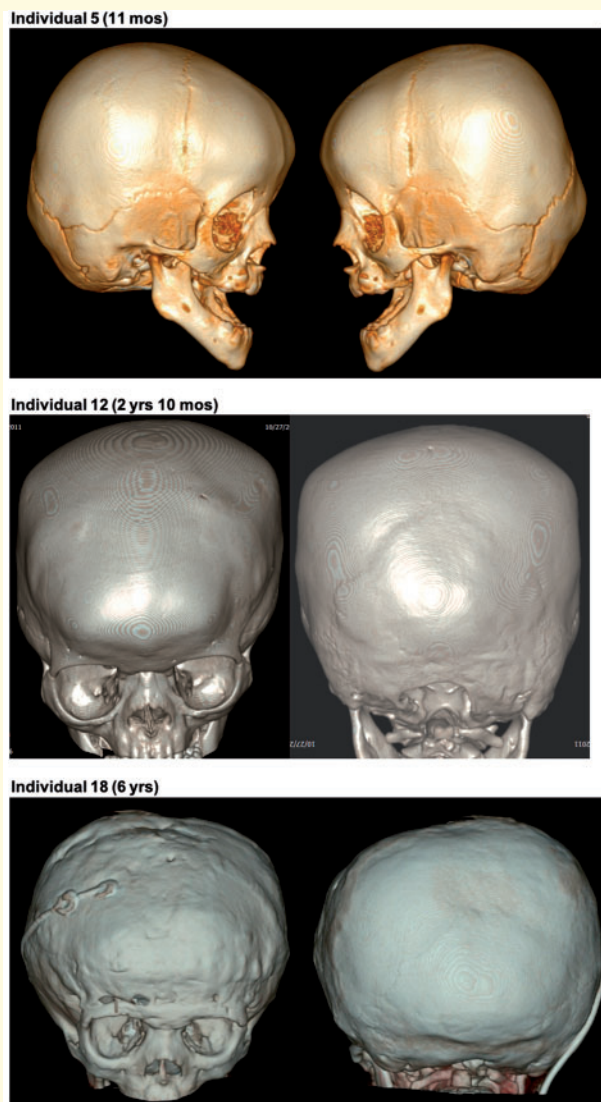


Figure 3 3D CT scans indicating craniosynostosis in individuals with C-terminal truncating mutations in *MN1*. For Individual 5, images show bilateral partial craniosynostosis of squamosal, frontosphenoid and coronal sutures. For Individuals 12 and 18, images show closure of the metopic, coronal and sagittal sutures and partial closure of lambdoid sutures. The images of Individual 18 are subsequent to fronto-orbital advancement surgery and placement of a ventriculoperitoneal shunt.

individuals unlikely to have severe paediatric disease, five loss-of-function *MN1* variants have been reported (each with an allele count of one; data accessed May 2019), all of which are positioned >55 bp upstream of the 3' end of exon 1 (Fig. 1), suggesting all would provoke nonsense-mediated mRNA decay, in contrast to the more C-terminal variants. In addition to the C-terminal truncating variants in MCTT patients, we also identified, through trio WES, three *de novo* truncating variants in the N-terminal third of *MN1*, in patients with a phenotype partly overlapping, but distinct from that of MCTT syndrome: p.(Ser179*) in

Individual 24 (with dyspraxia, mild conductive hearing loss, facial asymmetry and submucous cleft palate); p.(Pro365Thrfs*120) in Individual 25 (with social interaction issues, speech delay, mild conductive hearing loss and a prominent nose); and p.(Ser472*) in Individual 26 (with speech delay, mild conductive hearing loss and non-specific facial features) (Figs 1 and 6 and Supplementary Table 1). These three variants are also predicted to induce nonsense-mediated mRNA decay. Although all three patients had conductive hearing loss and a range of speech defects, none had significant intellectual disability or a facial gestalt reminiscent of MCTT syndrome.

We also report here the first known microdeletion harbouring *MN1* but no other genes (130 kb at chr22:287 1057 465–287 2357 360), which occurred *de novo* in Individual 27 (with microcephaly, intellectual disability, speech and motor delays and mildly dysmorphic facial features) (Fig. 6 and Supplementary Table 1). In the DECIPHER (Firth *et al.*, 2009) database and the literature, large deletions containing *MN1* and other genes have been described in individuals with variable neurodevelopmental and facial anomalies. The most frequent findings reported in these individuals are cleft or high-arched palate, micro- and/or retrognathia, hypertelorism, either depressed or prominent nasal bridge, low set and/or dysplastic ears, hypoplastic corpus callosum, mild to moderate developmental delay and intellectual disability including delayed speech (we include here the cases described in: Bruder *et al.*, 2001; Barbi *et al.*, 2002; Said *et al.*, 2011; Davidson *et al.*, 2012; Beck *et al.*, 2015; Breckpot *et al.*, 2016) and DECIPHER Individuals 999, 4110, 290785, 294749 and 331398, for a total of 19 individuals). Although some of these features are observed in MCTT syndrome, the majority (16/19) of these individuals have deletions >2 Mb and that contain at least 10 MIM genes, making it difficult to judge the contribution of *MN1* haploinsufficiency to the phenotype. For one of the smallest previously reported deletions harbouring *MN1*, DECIPHER 999 (Individual 28 here; see Supplementary Table 1 for clinical details), facial features are shown in Fig. 6 (photographs have not been previously published). Based on photographs of Individuals 27 and 28 and those available in the literature, individuals with deletions of *MN1* do not exhibit a consistent facial gestalt, and they do not resemble individuals with MCTT syndrome. Furthermore, review of brain imaging for Individuals 24, 27 and 28 did not reveal RES or the other findings frequently observed in patients with C-terminal truncating variants (Figs 4 and 5). Collectively, the above data suggest that haploinsufficiency for *MN1* may lead to neurodevelopmental anomalies, palatal defects and facial dysmorphisms with variable expressivity and penetrance but without significant similarity to the craniofacial gestalt or brain malformations of MCTT syndrome. We speculate that these differences are due to the stable expression of C-terminally truncated *MN1* protein in the latter, which may act in a dominant negative or gain-of-function manner.

Table 2 Brain imaging features in individuals with C-terminal truncating MNI variants

Feature	Prevalence
RES	8/10
Cerebellar dysplasia (other than RES)	4/10
Perisylvian polymicrogyria	9/10
Subcortical heterotopia	2/11
Ventriculomegaly	3/11
Thick rostral corpus callosum	6/11
Hypoplastic olfactory bulbs	4/8
Persistent trigeminal artery	7/10
Prominent posterior clinoid process	7/10
Hypertelorism	10/11

The frequencies are based uniquely on MRIs that were reviewed as a series at one centre.

Discussion

MNI: a poorly characterized gene implicated in craniofacial skeletal development

MNI was initially named because of its disruption by a balanced translocation in a meningioma (Lekanne Deprez *et al.*, 1995), and at the same time was identified in translocations in myeloproliferative disorders (Buijs *et al.*, 1995), resulting in fusions with *TEL*, encoding an ETS family transcription factor (now known as *ETV6*; MIM 600618). While the relevance of the initial association with meningioma has remained unclear, MNI has been strongly associated with leukaemia. Overexpression of

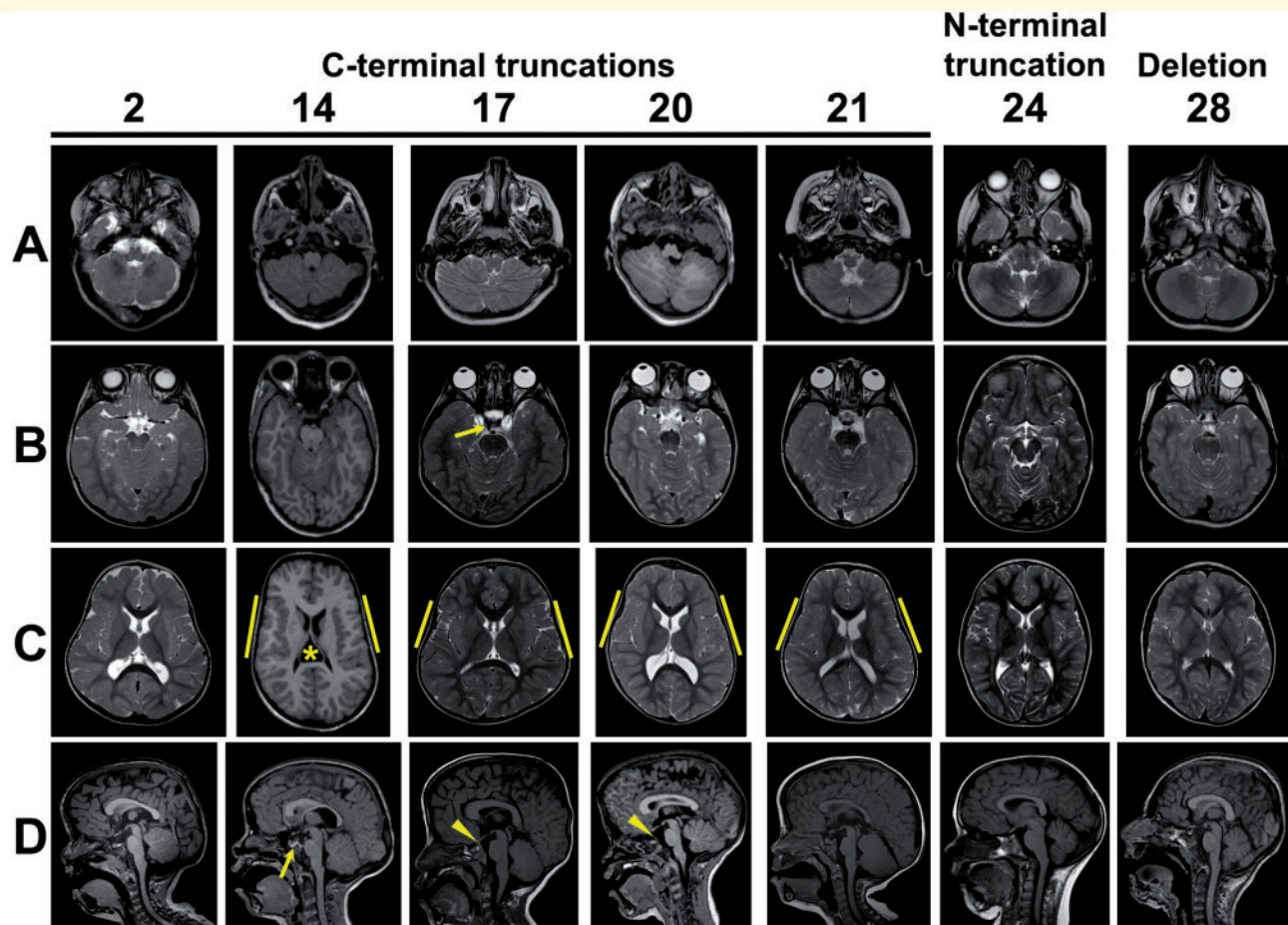


Figure 4 Brain findings in patients with C-terminal truncating MNI variants. (A) Inferior cerebellum (axial view): foliar dysplasia with indistinct vermis and abnormal folia crossing the midline (Individuals 2, 14, 17, 20, 21); normal inferior cerebellar anatomy (Individuals 24 and 28). (B) Superior cerebellum (axial view): small (Individuals 17, 20 and 21) or almost absent (Individuals 2 and 14) vermis with abnormal folia crossing the midline especially ventrally; normal superior cerebellar anatomy with intact vermis (Individuals 24 and 28). Arrow in Individual 17 indicates persistent trigeminal artery. (C) Insula (axial view): polymicrogyria inferior to yellow bars (Individuals 14, 17, 20 and 21), normal appearance (Individuals 2, 24 and 28). Note that Individual 14 has a cavum velum interpositum (asterisk) and all individuals with C-terminal truncating variants have unusual head shape with bitemporal narrowing. (D) Midline (sagittal view): Tall, flat forehead and thickened rostral corpus callosum (Individuals 2, 14, 17, 20 and 21), abnormal vermis lobulation with indistinct primary and horizontal fissures (Individuals 2, 14, 17, 20 and 21), persistent trigeminal artery (arrow in Individual 14) and prominent posterior clinoid process (arrowheads in Individuals 17 and 20).

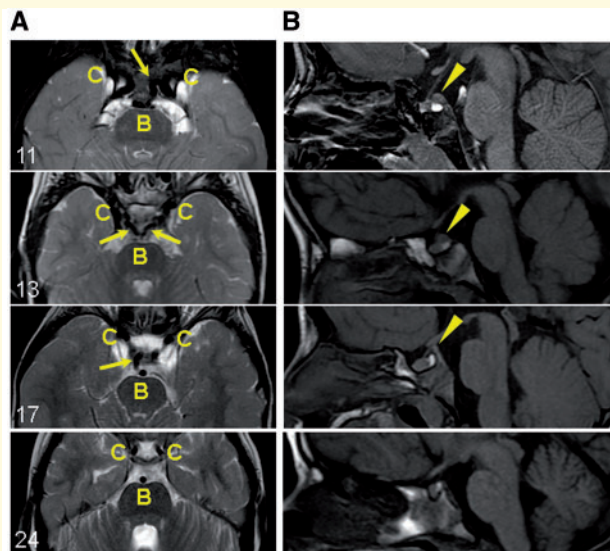


Figure 5 Persistent trigeminal artery and prominent posterior clinoid process in patients with C-terminal truncating MN1 variants. (A) Carotid and basilar arteries (axial view): Persistent trigeminal artery flow-voids (dark signal) connecting the carotid (C) and basilar (B) artery flow-voids (arrows). The persistent trigeminal arteries are unilateral in Individuals 11 and 17, and bilateral in Individual 13. Individual 24 with an early truncating variant does not have persistent trigeminal arteries (shown for comparison). (B) Prominent posterior clinoid process (sagittal view): abnormal tissue just superior to the posterior pituitary bright spot and continuous with the posterior clinoid process (arrow-heads). Individual 24 without the abnormal tissue is shown for comparison.

wild-type *MN1* in mice results in acute myeloid leukaemia (AML) or myeloproliferative disease (Carella *et al.*, 2007; Heuser *et al.*, 2007) and elevated *MN1* expression is a marker of poor prognosis of AML in humans (Heuser *et al.*, 2006). Note that none of the patients reported here have cancer. *MN1* contains no recognized protein domains or homology to other proteins, making predictions of its molecular functions difficult. It localizes to the nucleus (Buijs *et al.*, 2000) and contains proline-rich regions and poly-glutamine tracts. *In vitro* reporter assays have shown that *MN1* can act as a transcriptional activator, synergizing in some contexts with retinoic acid receptors, nuclear receptor coactivators or p300 (Buijs *et al.*, 2000; van Wely *et al.*, 2003; Sutton *et al.*, 2005; Liu *et al.*, 2008; Zhang *et al.*, 2009), but *MN1* is not thought to directly bind DNA (van Wely *et al.*, 2003; Meester-Smoor *et al.*, 2007). Further evidence for a role in transcriptional regulation comes from ChIP-Seq (chromatin immunoprecipitation-sequencing) studies that identified co-occupancy of *MN1* and the HOX co-factor MEIS1 (MIM 601739) at chromatin regions containing putative direct target genes of both factors in leukaemic cells (Heuser *et al.*, 2011).

Structure-function studies have highlighted several broad regions of *MN1*, in either the N- or C-terminal halves of the

protein, involved in its ability to regulate haematopoietic cell fate and leukaemogenesis (Kandilci *et al.*, 2013; Lai *et al.*, 2014); however, to the best of our knowledge, no specific activity has been attributed to the 60 C-terminal amino acids encoded by exon 2. Interestingly, within exon 2, the final 20 amino acids (which are fully or partially deleted in all individuals with MCTT syndrome) are particularly highly conserved across vertebrate species (Fig. 1B). A key area for future studies will involve investigation of the molecular function of this highly conserved C-terminus of *MN1*.

During embryonic development of animal models, *MN1* is expressed in restricted domains relevant to the tissues affected in MCTT syndrome. The zebrafish orthologue *mn1b* is expressed in the neural plate (presumptive central nervous system) during gastrulation and subsequently is strongly expressed in the midbrain and hindbrain during segmentation stages followed by additional expression in the telencephalon and pharyngeal arches (ZFIN database). In mouse embryos between embryonic day (E)9.5 and 12.5, the major sites of *Mn1* expression are the frontonasal prominences, pharyngeal arches and brain, especially the ventricular zone (Liu *et al.*, 2008). At E14.5, strongest expression occurs in the mantle zone of the forebrain, with expression also observed in other regions of the brain (lateral midbrain, cerebellum, pons), head mesenchyme, the palatal shelf and the developing digits and axial skeleton (Eurexpress database) (Diez-Roux *et al.*, 2011). Homozygous *Mn1*-null mice die shortly after birth due to clefting of the secondary palate (Meester-Smoor *et al.*, 2005; Liu *et al.*, 2008). These mice also display agenesis or hypoplasia of several bones of the ventral and lateral walls of the skull and thinning of bones of the skull roof, but no axial or appendicular skeletal defects nor anomalies of internal organs (Meester-Smoor *et al.*, 2005). In a genome-wide study of single nucleotide polymorphisms associated with variation in skull and mandible shape in mice, *Mn1* was contained in the locus with the largest effect size (Pallares *et al.*, 2015). Also, during evolution the *MN1* gene is suspected to have arisen at the base of the bony vertebrates (Pallares *et al.*, 2015). *Mn1* expression increases during differentiation of primary osteoblasts, and *Mn1* is necessary for the proliferation, differentiation and several functions of this cell type (Zhang *et al.*, 2009). Collectively these data suggest that *MN1* plays an essential and conserved role in development of the bones of the skull. Although the molecular function of the *MN1* alleles identified in MCTT syndrome remains unclear (see below), the above studies are consistent with the finding that alterations in skull and facial shape are a constant feature of MCTT syndrome.

Mutations in *MN1* cause partial rhombencephalosynapsis

In addition to distinctive craniofacial features, several MCTT syndrome patients have a focal variant of RES,

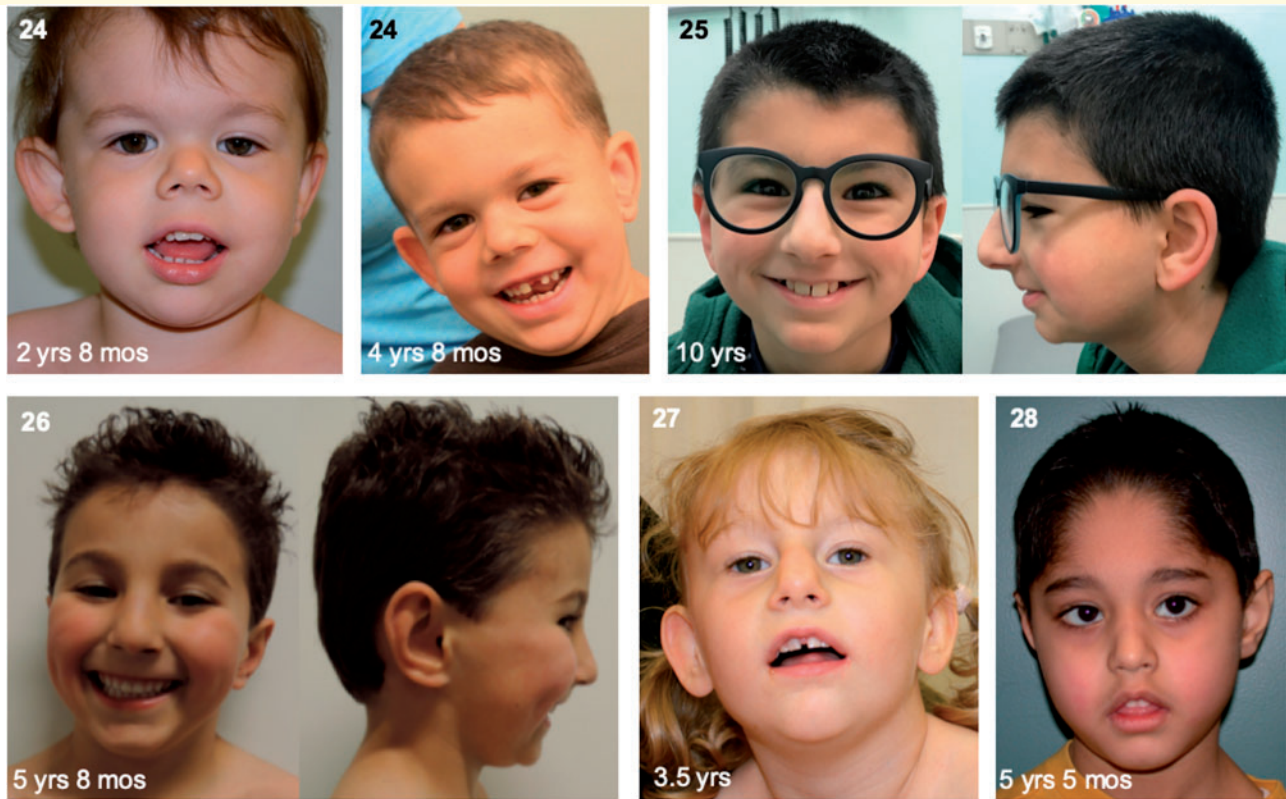


Figure 6 Facial features of individuals with N-terminal truncating mutations in *MNI* or whole deletions of *MNI*. Individual identification numbers are indicated at the top left of each panel.

usually involving less than half of the vermis. Interestingly, previously reported individuals with RES can also present craniofacial features such as high forehead, flat midface and low-set ears (Tully *et al.*, 2012), which are frequent features in patients with MCTT syndrome. No consistent causes of RES have been reported and no animal models exist. Possible RES has been reported in a single individual with a *de novo* deleterious *CHAMP1* variant (Hempel *et al.*, 2015), in one of two siblings with a frameshift mutation in *ZIC1* (Vandervore *et al.*, 2018), in two siblings with a 7 bp *ZIC2* deletion (Ramocki *et al.*, 2011), and in a foetus with a *de novo* missense variant in *ADGRL2* (Vezain *et al.*, 2018); however, the published imaging is inadequate to unambiguously establish the RES diagnosis in the above cases. In addition, we did not identify likely pathogenic variants in these genes in exome data from 59 individuals with RES (Aldinger *et al.*, 2018) and no additional families have been published, so *CHAMP1*, *ZIC1*, *ZIC2* and *ADGRL2* are unlikely to be strongly associated with RES. Therefore, identifying a role for *MNI* in the pathogenesis of RES is a major advance in our understanding of this malformation. Several theories for the developmental basis of RES have been proposed, particularly perturbed dorsal midline patterning due to the association of RES with holoprosencephaly and other midline brain defects in some patients (Ishak *et al.*, 2012). Unfortunately, *MNI* does not have a known role in these

processes, so further understanding of RES will require additional functional work in human and animal model systems.

Clinical implications

The diagnosis of MCTT syndrome has important clinical implications. It is caused by *de novo* variants, making the recurrence risk low. Based on the 22 individuals with germline C-terminal mutations in our cohort, the range of neurodevelopmental outcome is broad, but all individuals require educational and therapy support, particularly for communication, and are not expected to be fully independent in adulthood. MCTT syndrome individuals are at risk for craniosynostosis, which may result in increased intracranial pressure. In addition, they have a high frequency of persistent trigeminal artery, which can affect surgical approaches to the skull base and pituitary. Finally, our comparison of the MCTT syndrome phenotype with that of patients harbouring more N-terminal truncating variants indicates that the latter group are likely to have less severe neurodevelopmental outcomes.

Conclusion

In summary, we have identified *de novo* C-terminal truncating mutations in *MNI* as the cause of a severe and

recognizable syndrome involving neurodevelopmental deficits and dysmorphic craniofacial features that is distinct from the variable and incompletely penetrant phenotypes associated with haploinsufficiency of this gene. Our findings will improve genetic counselling options for families of patients with *MN1* variants and will motivate further basic research into the molecular roles of *MN1*, in particular regarding the function of its highly conserved C-terminus, and into the poorly defined developmental roles of *MN1*, especially in the context of CNS and craniofacial skeletal development. Importantly, our work opens the door to understanding the mechanisms underlying RES, a poorly understood cerebellar malformation.

Acknowledgements

We are extremely grateful to the families for their participation. We thank David Sweetser, Claire Redin and Michael E. Talkowski for initial discussions, and Shelin Adam who provided genetic counselling and coordinated J.M.F.'s research into pathogenic genomic variants.

Funding

This work was supported by grants from the Université Sorbonne Paris-Cité Pôle de recherche et d'enseignement supérieur (project number SPC/JFG/2013-031), the Agence Nationale de la Recherche [CranioRespiro project and 'Investissements d'avenir' program (ANR-10-IAHU-01)], MSDAvenir (DevoDecode project), E-Rare (CRANIRARE project), The Society for the Relief of Disabled Children, Medix Medical Services Asia, the Nachwuchskommission of the Charité Berlin (Rahel-Hirsch scholarship) to N.E., the German Research Foundation (DFG; SFB1315 to A.M.K. and LE 4223/1 to D.L.), the NIH Eunice Kennedy Shriver National Institute of Child Health and Human Development (U54HD083091, Genetics Core) to D.D., the NIH National Institute of Neurological Diseases and Stroke (R01NS050375) to W.B.D., the NIH National Human Genome Research Institute (HG009599) to J.T.S., the NIH National Human Genome Research Institute and the NIH National Heart, Lung and Blood Institute (grants UM1 HG006493 and U24 HG008956) to M.J.B. and D.A.N. (for sequencing provided by the University of Washington Center for Mendelian Genomics) and by private donations from families to D.D. The content is solely the responsibility of the authors and does not necessarily represent the official views of the National Institutes of Health. F.R.Z. was supported by a Canadian Institute of Health Research fellowship and W.T.G. was supported by the BC Children's Hospital Research Institute through its intramural IGAP Clinician Scientist Award program. The DDD study presents independent research commissioned by the Health Innovation Challenge Fund (grant number HICF-1009-003). This study makes use of DECIPHER

(<http://decipher.sanger.ac.uk>), which is funded by the Wellcome. See Deciphering Developmental Disorders Study (2015) or www.ddduk.org/access.html for full acknowledgement.

Competing interests

M.T.C, S.Y., F.M., I.M.W. and L.B.H. are employees of GeneDx, Inc. C.G.-J. is a full-time employee of the Regeneron Genetics Center and receives stock options as part of compensation.

Supplementary material

Supplementary material is available at *Brain* online.

References

- Acuna-Hidalgo R, Veltman JA, Hoischen A. New insights into the generation and role of de novo mutations in health and disease. *Genome Biol* 2016; 17: 241.
- Aldinger KA, Dempsey JC, Tully HM, Grout ME, Mehaffey MG, Dobyns WB, et al. Rhombencephalosynapsis: Fused cerebellum, confused geneticists. *Am J Med Genet C Semin Med Genet* 2018; 178: 432–9.
- Barbi G, Rossier E, Vossbeck S, Hummler H, Lang D, Flock F, et al. Constitutional de novo interstitial deletion of 8 Mb on chromosome 22q12.1-12.3 encompassing the neurofibromatosis type 2 (NF2) locus in a dysmorphic girl with severe malformations. *J Med Genet* 2002; 39: E6.
- Beck M, Peterson JF, McConnell J, McGuire M, Asato M, Losee JE, et al. Craniofacial abnormalities and developmental delay in two families with overlapping 22q12.1 microdeletions involving the *MN1* gene. *Am J Med Genet A* 2015; 167A: 1047–53.
- Breckpot J, Anderlid B-M, Alanay Y, Blyth M, Brahimi A, Duban-Bedu B, et al. Chromosome 22q12.1 microdeletions: confirmation of the *MN1* gene as a candidate gene for cleft palate. *Eur J Hum Genet* 2016; 24: 51–8.
- Bruder CE, Hirvelä C, Tapia-Paez I, Fransson I, Segraves R, Hamilton G, et al. High resolution deletion analysis of constitutional DNA from neurofibromatosis type 2 (NF2) patients using microarray-CGH. *Hum Mol Genet* 2001; 10: 271–82.
- Buijs A, Sherr S, van Baal S, van Bezouw S, van der Plas D, Geurts van Kessel A, et al. Translocation (12;22) (p13;q11) in myeloproliferative disorders results in fusion of the ETS-like *TEL* gene on 12p13 to the *MN1* gene on 22q11. *Oncogene* 1995; 10: 1511–9.
- Buijs A, van Rompaey L, Molijn AC, Davis JN, Vertegeal AC, Potter MD, et al. The *MN1-TEL* fusion protein, encoded by the translocation (12;22)(p13;q11) in myeloid leukemia, is a transcription factor with transforming activity. *Mol Cell Biol* 2000; 20: 9281–93.
- Carella C, Bonten J, Sirma S, Kranenburg TA, Terranova S, Klein-Geltink R, et al. *MN1* overexpression is an important step in the development of inv(16) AML. *Leukemia* 2007; 21: 1679–90.
- Choi M, Scholl UI, Ji W, Liu T, Tikhonova IR, Zumbo P, et al. Genetic diagnosis by whole exome capture and massively parallel DNA sequencing. *Proc Natl Acad Sci USA* 2009; 106: 19096–101.
- Davidson TB, Sanchez-Lara PA, Randolph LM, Krieger MD, Wu S-Q, Panigrahy A, et al. Microdeletion del(22)(q12.2) encompassing the facial development-associated gene, *MN1* (meningioma 1) in a child with Pierre-Robin sequence (including cleft palate) and neurofibromatosis 2 (NF2): a case report and review of the literature. *BMC Med Genet* 2012; 13: 19.

- Deciphering Developmental Disorders Study. Large-scale discovery of novel genetic causes of developmental disorders. *Nature* 2015; 519: 223–8.
- Deciphering Developmental Disorders Study. Prevalence and architecture of de novo mutations in developmental disorders. *Nature* 2017; 542: 433–8.
- Diez-Roux G, Banfi S, Sultan M, Geffers L, Anand S, Rozado D, et al. A high-resolution anatomical atlas of the transcriptome in the mouse embryo. *PLoS Biol* 2011; 9: e1000582.
- Farwell KD, Shahmirzadi L, El-Khechen D, Powis Z, Chao EC, Tippin Davis B, et al. Enhanced utility of family-centered diagnostic exome sequencing with inheritance model-based analysis: results from 500 unselected families with undiagnosed genetic conditions. *Genet Med* 2015; 17: 578–86.
- Firth HV, Richards SM, Bevan AP, Clayton S, Corpas M, Rajan D, et al. DECIPHER: database of chromosomal imbalance and phenotype in humans using ensembl resources. *Am J Hum Genet* 2009; 84: 524–33.
- Friedman J, Adam S, Arbour L, Armstrong L, Baross A, Birch P, et al. Detection of pathogenic copy number variants in children with idiopathic intellectual disability using 500 K SNP array genomic hybridization. *BMC Genomics* 2009; 10: 526.
- Friedman JM, Baross A, Delaney AD, Ally A, Arbour L, Armstrong L, et al. Oligonucleotide microarray analysis of genomic imbalance in children with mental retardation. *Am J Hum Genet* 2006; 79: 500–13.
- Gurovich Y, Hanani Y, Bar O, Nadav G, Fleischer N, Gelbman D, et al. Identifying facial phenotypes of genetic disorders using deep learning. *Nat Med* 2019; 25: 60–4.
- Hempel M, Cremer K, Ockeloen CW, Lichtenbelt KD, Herkert JC, Denecke J, et al. De Novo mutations in CHAMP1 cause intellectual disability with severe speech impairment. *Am J Hum Genet* 2015; 97: 493–500.
- Heuser M, Argiropoulos B, Kuchenbauer F, Yung E, Piper J, Fung S, et al. MN1 overexpression induces acute myeloid leukemia in mice and predicts ATRA resistance in patients with AML. *Blood* 2007; 110: 1639–47.
- Heuser M, Beutel G, Krauter J, Döhner K, von Neuhoff N, Schlegelberger B, et al. High meningioma 1 (MN1) expression as a predictor for poor outcome in acute myeloid leukemia with normal cytogenetics. *Blood* 2006; 108: 3898–905.
- Heuser M, Yun H, Berg T, Yung E, Argiropoulos B, Kuchenbauer F, et al. Cell of origin in AML: susceptibility to MN1-induced transformation is regulated by the MEIS1/AbdB-like HOX protein complex. *Cancer Cell* 2011; 20: 39–52.
- Ishak GE, Dempsey JC, Shaw DWW, Tully H, Adam MP, Sanchez-Lara PA, et al. Rhombencephalosynapsis: a hindbrain malformation associated with incomplete separation of midbrain and forebrain, hydrocephalus and a broad spectrum of severity. *Brain* 2012; 135: 1370–86.
- Jansen S, Geuer S, Pfundt R, Brough R, Ghongane P, Herkert JC, et al. De Novo truncating mutations in the last and penultimate exons of PPM1D cause an intellectual disability syndrome. *Am J Hum Genet* 2017; 100: 650–8.
- Kandilci A, Surtel J, Janke L, Neale G, Terranova S, Grosveld GC. Mapping of MN1 sequences necessary for myeloid transformation. *PLoS ONE* 2013; 8: e61706.
- Lai CK, Moon Y, Kuchenbauer F, Starczynowski DT, Argiropoulos B, Yung E, et al. Cell fate decisions in malignant hematopoiesis: leukemia phenotype is determined by distinct functional domains of the MN1 oncogene. *PLoS ONE* 2014; 9: e112671.
- Lekanne Deprez RH, Riegman PH, Groen NA, Warringa UL, van Biezen NA, Molijn AC, et al. Cloning and characterization of MN1, a gene from chromosome 22q11, which is disrupted by a balanced translocation in a meningioma. *Oncogene* 1995; 10: 1521–8.
- Lelieveld SH, Reijnders MRF, Pfundt R, Yntema HG, Kamsteeg E-J, de Vries P, et al. Meta-analysis of 2,104 trios provides support for 10 new genes for intellectual disability. *Nat Neurosci* 2016; 19: 1194–6.
- Liu W, Lan Y, Pauws E, Meester-Smoor MA, Stanier P, Zwarthoff EC, et al. The Mn1 transcription factor acts upstream of Tbx22 and preferentially regulates posterior palate growth in mice. *Development* 2008; 135: 3959–68.
- Louie RJ, Tan QK-G, Gilner JB, Rogers RC, Younge N, Wechsler SB, et al. Novel pathogenic variants in FOXP3 in fetuses with echogenic bowel and skin desquamation identified by ultrasound. *Am J Med Genet A* 2017; 173: 1219–25.
- Meester-Smoor MA, Molijn AC, Zhao Y, Groen NA, Groffen CAH, Boogaard M, et al. The MN1 oncoprotein activates transcription of the IGFBP5 promoter through a CACCC-rich consensus sequence. *J Mol Endocrinol* 2007; 38: 113–25.
- Meester-Smoor MA, Vermeij M, van Helmond MJL, Molijn AC, van Wely KHM, Hekman ACP, et al. Targeted disruption of the Mn1 oncogene results in severe defects in development of membranous bones of the cranial skeleton. *Mol Cell Biol* 2005; 25: 4229–36.
- Nagy E, Maquat LE. A rule for termination-codon position within intron-containing genes: when nonsense affects RNA abundance. *Trends Biochem Sci* 1998; 23: 198–9.
- O'uchi E, O'uchi T. Persistent primitive trigeminal arteries (PTA) and its variant (PTAV): analysis of 103 cases detected in 16,415 cases of MRA over 3 years. *Neuroradiology* 2010; 52: 1111–9.
- Pallares LF, Carbonetto P, Gopalakrishnan S, Parker CC, Ackert-Bicknell CL, Palmer AA, et al. Mapping of craniofacial traits in outbred mice identifies major developmental genes involved in shape determination. *PLoS Genet* 2015; 11: e1005607.
- Poirier K, Hubert L, Viot G, Rio M, Billuart P, Besmond C, et al. CSNK2B splice site mutations in patients cause intellectual disability with or without myoclonic epilepsy. *Hum Mutat* 2017; 38: 932–941.
- Ramocki MB, Scaglia F, Stankiewicz P, Belmont JW, Jones JY, Clark GD. Recurrent partial rhombencephalosynapsis and holoprosencephaly in siblings with a mutation of ZIC2. *Am J Med Genet A* 2011; 155A: 1574–80.
- Rossi M, El-Khechen D, Black MH, Farwell Hagman KD, Tang S, Powis Z. Outcomes of diagnostic exome sequencing in patients with diagnosed or suspected autism spectrum disorders. *Pediatr Neurol* 2017; 70: 34–43.e2.
- Said E, Cuschieri A, Vermeesch J, Fryns JP. Toriello-Carey syndrome with a 6Mb interstitial deletion at 22q12 detected by array CGH. *Am J Med Genet A* 2011; 155A: 1390–2.
- Sobreira N, Schiettecatte F, Valle D, Hamosh A. GeneMatcher: a matching tool for connecting investigators with an interest in the same gene. *Hum Mutat* 2015; 36: 928–30.
- Strauss KA, Gonzaga-Jauregui C, Brigatti KW, Williams KB, King AK, Van Hout C, et al. Genomic diagnostics within a medically underserved population: efficacy and implications. *Genet Med* 2018; 20: 31–41.
- Sutton ALM, Zhang X, Ellison TI, Macdonald PN. The 1,25(OH)2D3-regulated transcription factor MN1 stimulates vitamin D receptor-mediated transcription and inhibits osteoblastic cell proliferation. *Mol Endocrinol* 2005; 19: 2234–44.
- Tanaka AJ, Cho MT, Millan F, Juusola J, Retterer K, Joshi C, et al. Mutations in SPATA5 are associated with microcephaly, intellectual disability, seizures, and hearing loss. *Am J Hum Genet* 2015; 97: 457–64.
- Tully HM, Dempsey JC, Ishak GE, Adam MP, Curry CJR, Sanchez-Lara P, et al. Beyond Gómez-López-Hernández syndrome: recurring phenotypic themes in rhombencephalosynapsis. *Am J Med Genet A* 2012; 158A: 2393–406.
- Tully HM, Dempsey JC, Ishak GE, Adam MP, Mink JW, Dobyns WB, et al. Persistent figure-eight and side-to-side head shaking is a marker for rhombencephalosynapsis. *Mov Disord* 2013; 28: 2019–23.
- Van De Weghe JC, Rusterholz TDS, Latour B, Grout ME, Aldinger KA, Shaheen R, et al. Mutations in ARM9, which encodes a basal body protein, cause Joubert syndrome in humans and ciliopathy phenotypes in zebrafish. *Am J Hum Genet* 2017; 101: 23–36.

- Vandervore LV, Schot R, Hoogeboom AJM, Lincke C, de Coo IF, Lequin MH, et al. Mutated zinc finger protein of the cerebellum 1 leads to microcephaly, cortical malformation, callosal agenesis, cerebellar dysplasia, tethered cord and scoliosis. *Eur J Med Genet* 2018; 61: 783–9.
- van Wely KHM, Molijn AC, Buijs A, Meester-Smoor MA, Aarnoudse AJ, Hellemons A, et al. The MN1 oncoprotein synergizes with coactivators RAC3 and p300 in RAR-RXR-mediated transcription. *Oncogene* 2003; 22: 699–709.
- Vezain M, Lecuyer M, Rubio M, Dupé V, Ratié L, David V, et al. A de novo variant in ADGRL2 suggests a novel mechanism underlying the previously undescribed association of extreme microcephaly with severely reduced sulcation and rhombencephalosynapsis. *Acta Neuropathol Commun* 2018; 6: 109.
- White JJ, Mazzeu JF, Hoischen A, Bayram Y, Withers M, Gezirici A, et al. DVL3 alleles resulting in a -1 frameshift of the last exon mediate Autosomal-Dominant Robinow syndrome. *Am J Hum Genet* 2016; 98: 553–61.
- Zhang X, Dowd DR, Moore MC, Kranenburg TA, Meester-Smoor MA, Zwarthoff EC, et al. Meningioma 1 is required for appropriate osteoblast proliferation, motility, differentiation, and function. *J Biol Chem* 2009; 284: 18174–83.